ISBN: 978-628-95207-8-1. ISSN: 2414-6390. Digital Object Identifier: 10.18687/LACCEI2024.1.1.1922

Computational characterization of the magnetic force and stability of passive magnetic bearings with diametrical magnetization

Carlos A. Jiménez-Carballo, M.Sc[1], Marta Vilchez-Monge[2] and Gabriela Ortiz- León, Phd[3]
[1,2,3]Costa Rica Institute of Technology y, Costa Rica, carjimenez@itcr.ac.cr, gaby@itcr.ac.cr

Abstract– ***This paper examines the behavior of the axial component of magnetic force (F_z) and magnetic rigidity (k_z) in diametrically magnetized passive magnetic bearing configurations (PMBs). Numerical simulations of computational electromagnetism (CEM) based on the finite element method were performed to evaluate the behavior of F_z and k_z in various bearing configurations. First, an analytical expression of the magnetic field of a diametrically magnetized ring is presented, with the aim of identifying the parameters that determine the behavior of that field and hence the magnetic force. Additionally, F_z and k_z are analyzed based on the axial displacement of the internal magnets of systems formed by one or two diametrically magnetized bearings. Finally, the magnetic force and rigidity of three sets of two PMBs are compared. The first set is magnetized radially, the second set is magnetized axially, and the third set is magnetized diametrically.***

Keywords-- Diametrical magnetic bearing, passive magnetic bearing, magnetic field, magnetic stiffness, magnetic force.

I. Introduction

Currently, the Costa Rica Institute of Technology (TEC) is in the process of developing a ventricular assist device (VAD) [1]. In this project, a magnetic levitation system is being designed to ensure the stiffness of the VAD impeller, for which two passive magnetic bearings (PMBs) are necessary. A PMB is a machine element that generates the magnetic suspension of a rotor without any mechanical contact by using permanent magnets [2], [3]. These devices have multiple benefits; for example, they do not need energy to operate, have a very long-life spawn, and prevent friction between components. Because of this, they are used in electric motors that need magnetic support systems with low friction, such as VADs [4], [5], [6]. However, because PMBs use permanent magnets, these devices have significant drawbacks. For example, according to Earnshaw's theorem, it is impossible to suspend a ferromagnetic body in all of its degrees of freedom with this kind of bearing, which often requires the assistance of other types of bearings, such as hydrodynamic ones, to ensure stiffness [7]. They also have poor natural damping, which might lead to stiffness problems. Another disadvantage is that some physical parameters, such as PMB force or magnetic stiffness, need sophisticated calculations that require the use of a numerical method, such as the finite element method (FEM) [8].

Digital Object Identifier: (only for full papers, inserted by LACCEI).
ISSN, ISBN: (to be inserted by LACCEI).
DO NOT REMOVE

Different kinds of PMBs may be distinguished based on the orientation of the magnetization direction of the individual magnets that compose them. These may be categorized as axial, radial, radial-axial, and diametrical. As Yonnet [9] points out, in order to choose the best configuration for stiffness in a certain direction, axial force, or others, it is preferable to consider all feasible configurations and their key specifications before beginning to construct an instrument. Various studies on the behavior of magnetic force and magnetic stiffness for axial or radial PMBs can be found in the literature [9], [10], [11], [12], [13]; however, no studies on magnetic force or axial magnetic stiffness related to diametrical PMBs were found during the development of this research, nor was there evidence where the interaction between two or more diametrical PMBs was characterized according to the distance of separation between them.

The main goal of this research is to use FEM to characterize the axial magnetic stiffness k_z and the axial F_z component of the magnetic force between the internal and external magnets of either one or two PMBs, given that our VAD proposal will incorporate a levitation system composed of two PMBs. First, a brief explanation of the magnetic field generated by a diametrically magnetized permanent magnet is presented, with the aim of establishing a theoretical model that allows for the identification of the parameters that govern the behavior of such a field as well as a starting point for the verification of the numerical method used (section 2). Next, the behavior of k_z and F_z as a function of the axial displacement z for the configuration of one and two diametrically magnetized PMBs is studied (sections 3 and 4). Finally, the behavior of the magnetic force and magnetic stiffness of three systems of two PMBs is compared, the first radially magnetized, the second axially, and the third diametrically magnetized, in order to determine which system may be the best option for a magnetic stability system (section 5).

II. Magnetic field of a diametrically magnetized ring permanent magnet.

In order to establish the mathematical model and the parameters that define how this field behaves, this section gives a brief description of the magnetic field that a diametrically magnetized ring magnet produces. For this case, consider a ring with constant diametrical magnetization $\vec{M} = M\hat{y}$, such as the one shown in Fig. 1. It was tried to find a mathematical way

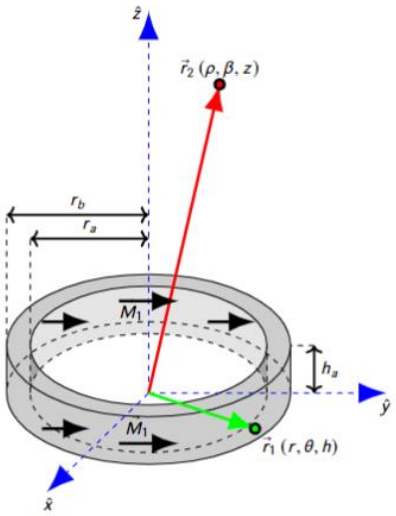

Fig. 1: Permanent ring with diametrical magnetization.

to describe the magnetic field $\vec{B}$ at a point located at $\vec{r}_2$ defined that is set by the coordinates ρ, β, and z.

According to Reitz [14], Van Tai Nguyen [15], and Fontana [16], the magnetic field produced by permanent magnets can be determined using the Couloumbian model, frequently referred to as the method of magnetic charge, that is

$$\vec{B} = \frac{\mu_0}{4\pi}\left[\int_{V_1} \frac{(\backslash Vec r_2 - \vec{r_1})}{|\vec{r_2} - \vec{r_1}|^3}\rho_M \mathrm{d}\, V_1 + \int_{A_1} \frac{(\vec{r_2} - \vec{r_1})}{|\vec{r_2} - \vec{r_1}|^3}\sigma_M \mathrm{d}\, A_1\right], \quad (1)$$

where the variable $\vec{r}_1$ is used to locate a point within the magnet, ρ_M and σ_M are known as the magnetic pole density and surface density of the magnetic pole intensity, respectively, and are determined

$$\rho_M = -\nabla \cdot \vec{M}, \quad (2)$$

$$\sigma_M = \vec{M} \cdot \vec{n}. \quad (3)$$

Ravaud also used the Couloumbian method to study the magnetic force between permanent magnets with axial or radial magnetization. The magnetization is normal to the surface in such cases [11], [12]. In this situation, the magnetization is constant, therefore $\rho_M = 0$. Additionally, the normal vector to the surface $\hat{n}$ produces an angle θ with $\vec{M}$, so $\sigma_M = M \sin\theta$, reducing (1) to

$$\vec{B} = \kappa \int_0^{2\pi} \int_0^{h_a} \left[\vec{\mathcal{B}}_b \mathrm{d}A_b - \vec{\mathcal{B}}_a \mathrm{d}A_a\right], \quad (4)$$

with

$$\overrightarrow{\mathcal{B}_\iota} = \frac{(\rho\cos\beta - r_i\cos\theta)\hat{x} + (\rho\sin\beta - r_i\sin\theta)\hat{y} + (z-h)\hat{z}}{[r_i^2 + \rho^2 - 2r_i\rho\cos(\beta-\theta) + (z-h)^2]^{3/2}}, \quad (5)$$

$$\kappa = \frac{\mu_0 M_1}{4\pi}, \quad (6)$$

$$\mathrm{d}A_i = r_i \sin\theta\, \mathrm{d}h\mathrm{d}\theta, \qquad \text{for } (i = a, b). \quad (7)$$

In this case, unlike Nguyen's [15] or Fontana's [16], cartesian unit vectors are used because they are constant throughout space, are easier to visualize and understand than cylindrical unit vectors, and are more common in scientific literature. As seen in (4), (5), (6) and (7), the determination of $\vec{B}$ is based on elliptic integrals, which may be solved numerically and analytically under certain conditions. For example, consider the situation of the ring's center line, that is, $\rho = 0$ and $\beta = 0$, for which (5) simplifies to

$$\overrightarrow{\mathcal{B}_\iota} = \frac{-r_i\cos\theta\hat{x} - r_i\sin\theta\,\hat{y} + (z-h)\hat{z}}{[r_i^2 + (z-h)^2]^{3/2}}. \quad (8)$$

Substituting (8) in (4) it can be shown that $B_x = B_z = 0$ and

$$B_y(z) = -\kappa\pi\left[\frac{z}{\sqrt{r_b^2 + z^2}} - \frac{z}{\sqrt{r_a^2 + z^2}}\right] - \kappa\pi\left[\frac{z - h_a}{\sqrt{r_a^2 + (z-h_a)^2}} - \frac{z - h_a}{\sqrt{r_b^2 + (z-h_a)^2}}\right]. \quad (9)$$

The Fig. 2 shows the behavior of B_y on the symmetry axis of a diametrically magnetized ring in the function of z. This figure presents a comparison of the results obtained from a numerical simulation carried out with the COMSOL Multiphysics program and the values of this component determined from the analytical expression (9), taking into account for both cases $r_a = 26$ mm, $r_b = 34$ mm, $h_a = 20$ mm, and $M_1 = 10$ kA/m. From which it can be verified that the results of the numerical simulation are reliable, as both results

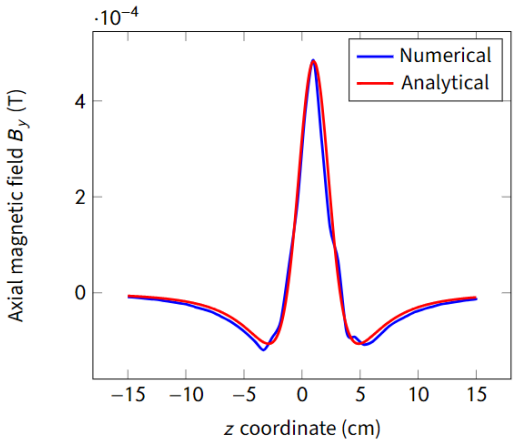

Fig. 2: A comparison of a numerical simulation performed using the COMSOL Multiphysics software and the analytical equation of B_y for a diametrically magnetized permanent magnet.

are almost identical. It can also be seen that, as expected, B_y is highest at the magnet's middle ($z = h_a/2 = 10$ mm), and it is the same whether $z = +z$ or $z = -z$.

III. Magnetic Force Between Two Rings with Constant Diametrical Magnetization

This section provides an explanation of the behavior of the axial magnetic force F_z and the magnetic stiffness k_z between two ring-shaped permanent magnets with constant diametrical magnetization (see Fig. 3). This configuration is known as the simplest PMB [17].

According to Camacho [18], the force that a permanent magnet with magnetic field $\overrightarrow{B_1}$ produces on another magnet with magnetization $\overrightarrow{M_2}$ is determined by

$$\vec{F} = \vec{\nabla} \int_V \vec{B}_1 \cdot \vec{M}_2 \mathrm{d}V_2 \,, \tag{10}$$

where $\mathrm{d}V_2$ is a volume element of the second magnet. In this case, the two permanent magnets are assumed to have constant diametrical magnetization, $\overrightarrow{M_1} = M_1\hat{y}$ and $\overrightarrow{M_2} = M_2\hat{j}$, as shown in Fig. 3; hence, according to (10), F_z is given by

$$F_z = M_2 \int_0^{2\pi} \int_{r_c}^{r_d} \left[B_{1y}(= z + h_b) - B_{1y}(z = z)\right] \rho d\rho \mathrm{d}\beta \,, \tag{11}$$

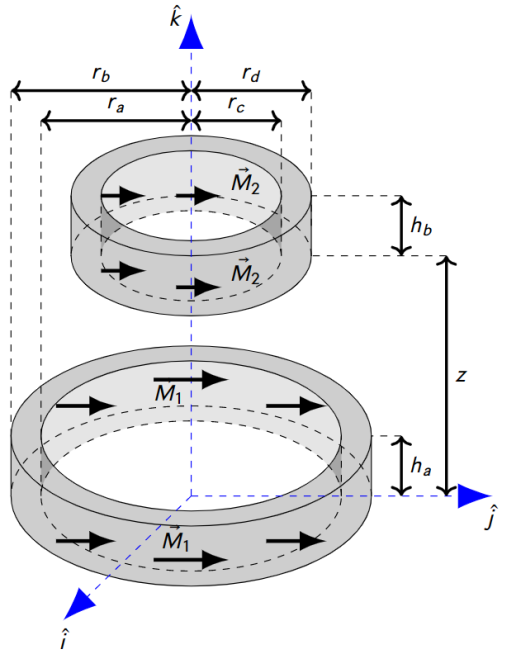

Fig. 3: This is a passive magnetic bearing with a simpler structure. It is made up of two rings of permanent magnets. In this case, the magnets have diametrical magnetization.

where B_{1y} is the magnetic field generated by the external magnet, whose expression is shown in (4). In addition, the axial magnetic stiffness k_z is given by the expression [17]

$$k_z \equiv -\frac{\partial F_z}{\partial z}.$$

where, in the case that $k_z > 0$, the system or configuration is said to be stable.

As F_z and k_z depend on B_{1y} (see (9)), the analytical determination of these expressions presents a considerable challenge; consequently, FEM, in particular the Comsol Multiphysics tool, was employed to estimate the variation of those physical values dependent on the axial displacement z. Fig. 4 shows how F_z changes as a function of z for two diametrically magnetized permanent magnets with different external radii r_d of the internal magnet. Also, Fig. 4 shows that the force exerted by the PMB's magnets has an effective range of $z = -10$ mm to $z = 10$ mm, with equilibrium being reached at $z = 0$; Outside of this range, F_z will always be null, despite the value that was assigned to r_d.

Fig. 5 shows how the axial magnetic stiffness k_z changes as a function of the axial displacement z of the internal magnet for different values of r_d. Results show axial stiffness increases as r_d goes up, which means that the space between the magnets gets smaller. At $z = 0$ m, the maximum values of k_z were found to be 1.193 N/m for $r_d = 24$ mm, 2.336 N/m for $r_d = 25$ mm, and 4.567 N/m for $r_d = 26$ mm.

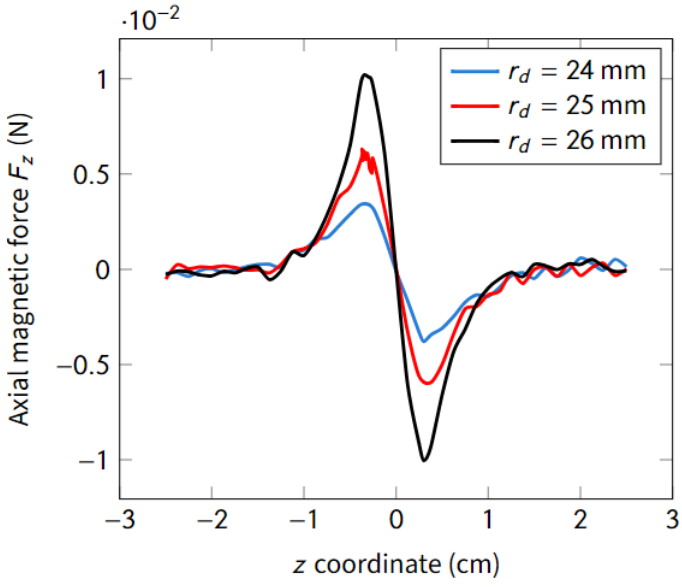

Fig. 4: Axial magnetic force exerted between two diametrically magnetized ring permanent magnets as a function of the axial displacement of the inner permanent ring magnets for various r_d values. In this case, $r_a = 26.6$ mm, $r_b = 34.8$ mm, $r_c = 13$ mm, $h_a = h_b = 5$ mm, and $M_1 = M_2 = 10$ kA/m.

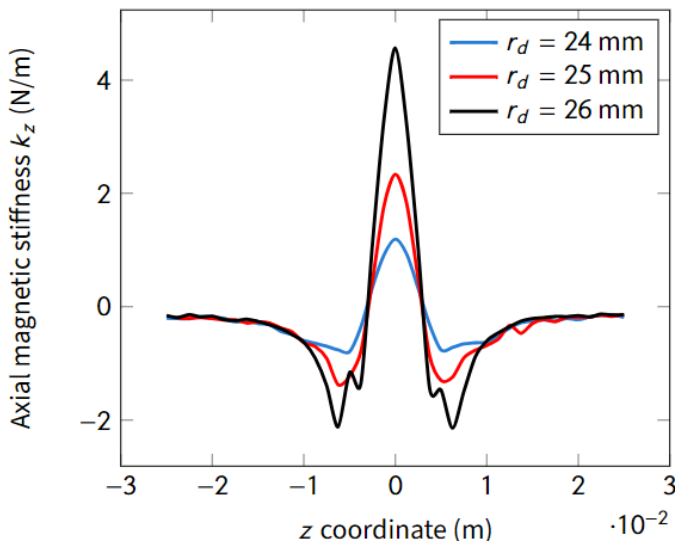

Fig. 5: Axial magnetic stiffness k_z function of the internal magnet's axial displacement z for varied values of r_d. It is considered for magnets $r_a = 26.6$ mm, $r_b = 34.8$ mm, $r_c = 13$ mm, $h_a = h_b = 5$ mm, and $M_1 = M_2 = 10$ kA/m.

Finally, it is important to remember that the geometric properties of the magnets specifically determine the shapes of the curves of k_z and F_z as a function of z. This is because in the Coulomb model, both the force and the stiffness are directly proportional to the magnetization values of the permanent magnets, as indicated by the expressions (11) and (12), respectively.

IV. Magnetic Force Between Two Diametrical Passive Magnetic Bearings

In this section, we will look at how the magnetic force that acts on the internal magnets of a configuration of two PMBs with diametrical magnetization changes. In this case, the distance between the bearings is $z_a = 95$ mm (this separation distance was chosen because the axial impeller for which the bearings will be used is approximately 100 mm long), and it is assumed that only the internal magnets of the bearings move, both in the same direction with respect to the z axis (see Fig. 6). Fig. 7 shows a cross-section of this arrangement, which shows the parameters that determine the size of the magnets in these bearings.

As mentioned in the previous section, the force between two permanent magnets cannot be determined analytically (see (11)) so this section will study the force and magnetic stiffness between two PMBs using FEM. Fig. 8 shows the axial component F_z of the magnetic force acting on the internal magnets of the PMBs as a function of the axial displacement z for different external radii r_d of the internal magnets, where a F_z behavior is observed similar to that of two permanent magnets shown in the previous section. For example, this force

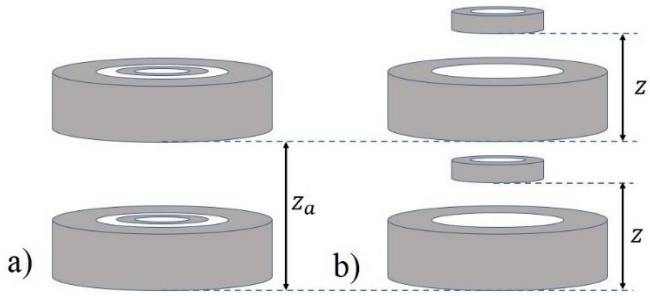

Fig. 6: Two passive magnetic bearings with diametrical magnetization. a) The internal magnets without axial displacement, b) The inner magnets of the cushions are displaced a distance z from the external magnets.

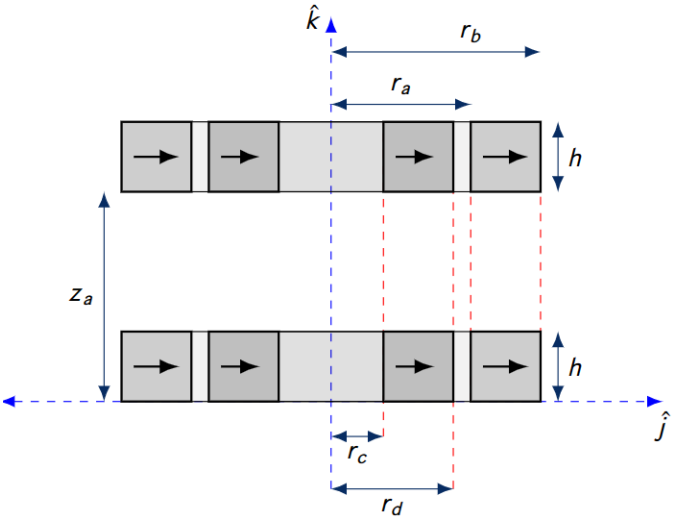

Fig. 7: Cross-section and arrangement of two diametrically magnetized PMBs.

is greater as r_d increases because the space between the magnets is smaller.

Also, for negative values of z the force is attractive and repulsive for positive values of z. The main difference is that the value of F_z is the double that is found for the case of one PMB, which is expected given that there are two PMBs separated by a distance of 95 mm, so the internal magnets of the bearings only feel the force of the external magnet of the bearing to which they belong, as a consequence of the results provided in the Fig. 4 where the force felt by a magnet is zero for $z < -10$ mm and $z > 10$ mm. Regarding the range of action of F_z, it can be seen that it is identical to that of one PMB; this is $-10 < z < 10$ mm, regardless of the value of r_d.

Axial magnetic stiffness k_z is shown in Fig. 9 as a function of axial displacement z for different values of r_d; similar to a PMB, the larger the value of r_d (and the smaller the distance between the magnets), the larger is k_z. Here, the maximum values of k_z are 2.303 N/m for $r_d = 24$ mm, 4.658 N/m for $r_d = 25$ mm, and 9.184 N/m for $r_d = 26$ mm.

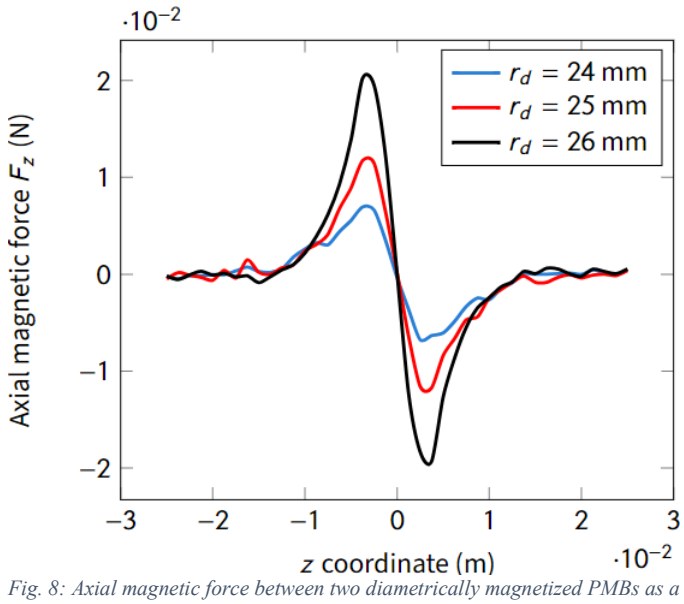

Fig. 8: Axial magnetic force between two diametrically magnetized PMBs as a function of the axial displacement of the inner permanent ring magnets for various r_d values. It is taken into account for magnets: r_a = 26.6 mm, r_b = 34.8 mm, r_c = 13 mm, $h_a = h_b$ = 5 mm, and $M_1 = M_2$ = 10 kA/m.

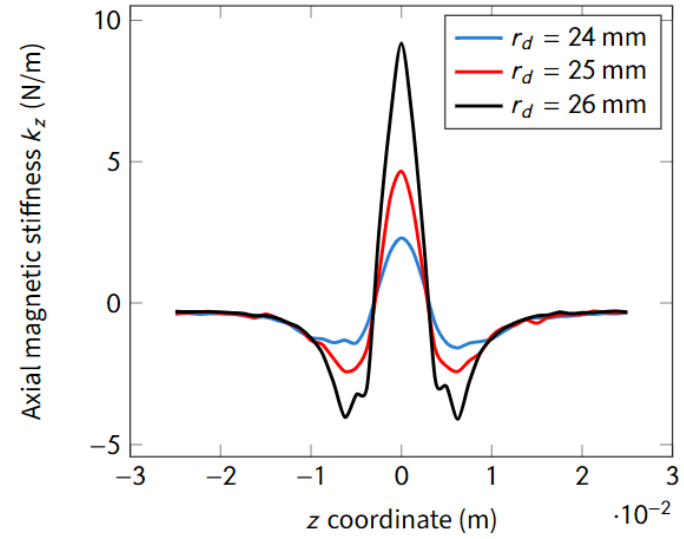

Fig. 9: Axial magnetic stiffness k_z between two diametrically magnetized PMBs as a function of the axial displacement of the inner permanent ring magnets for various r_d values. It is taken into account for magnets: r_a = 26.6 mm, r_b = 34.8 mm, r_c = 13 mm, $h_a = h_b$ = 5 mm, and $M_1 = M_2$ = 10 kA/m

As was already said, if two PMBs are more than $z_a = 10$ mm apart, they do not interact with each other. Because of this, we looked at how F_z and k_z changed when two PMBs were placed at different distances z_a apart. Fig. 10 shows the relationship between F_z and z when $z_a = 6.5, 12$ and 95 mm. It shows that if $z_a = 6.5$ mm, the maximum value of F_z is 13.2 mN, and the range of action of the force is between -20 mm and 20 mm. For the case where $z_a = 12$ mm, the maximum F_z was 17.9 mN, and the range of action of the force was also between -20 mm

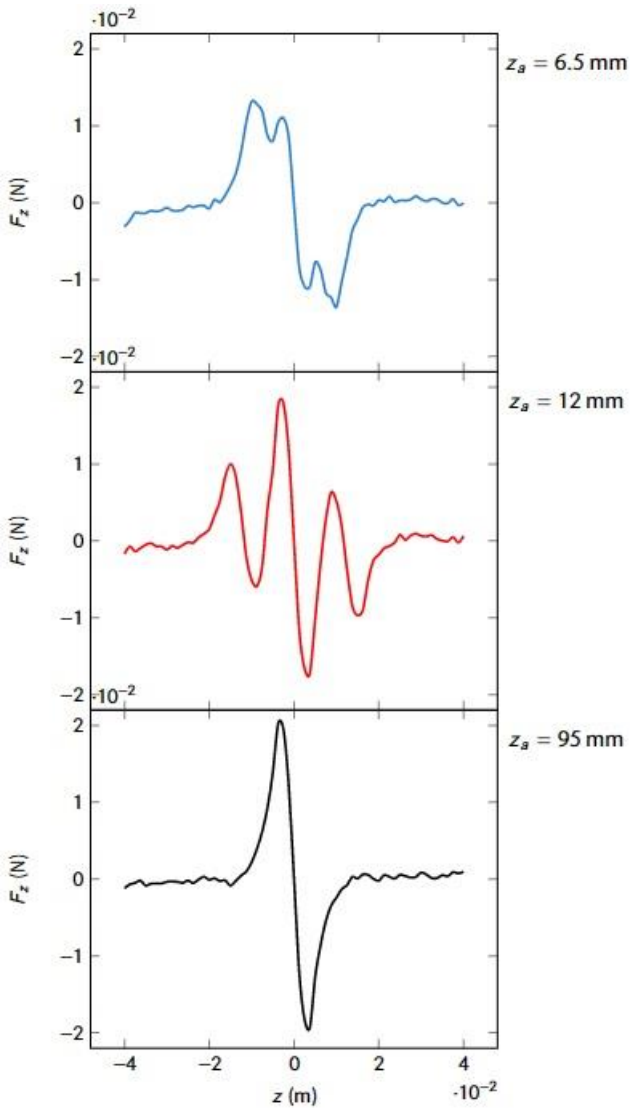

Fig. 10: Axial magnetic force between two diametrically magnetized PMBs as a function of the axial displacement of the inner permanent ring magnets for various z_a values. It is taken into account for magnets: r_a = 26.6 mm, r_b = 34.8 mm, r_c = 13 mm, r_d = 26 mm, h = 5 mm, and M = 10 kA/m.

and -20 mm. However, two more local maximums were found. This is because in those areas, only one of the two internal magnets is interacting with only one of the external magnets, similar to what is shown in Fig. 11. The Fig. 10 shows that the case $z_a = 95$ mm gave the highest value of F_z. This is because when the bearings with the same direction of magnetization are close to each other, the value of F_z decreases, which is due to the fact that when an internal magnet is in the middle of two external magnets at a small distance, one of them repels it and the other attracts it. For that reason, in the cases $z_a = 6.5$ mm and 12 mm, the maximum value of the force is lower.

Fig. 12 shows how k_z varies with z for different bearing separation distances z_a. In the cases of $z_a = 6.5$ mm and 12 mm, k_z is positive in three places, indicating that the design

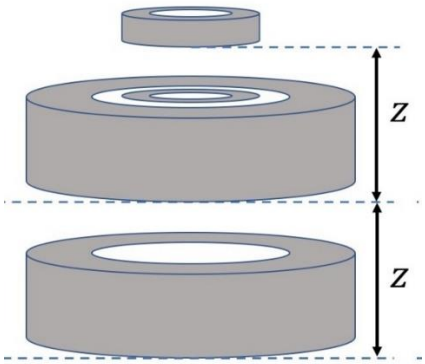

Fig. 11: Axial Displacement of Internal Magnets of PMBs, case $z = z_a$

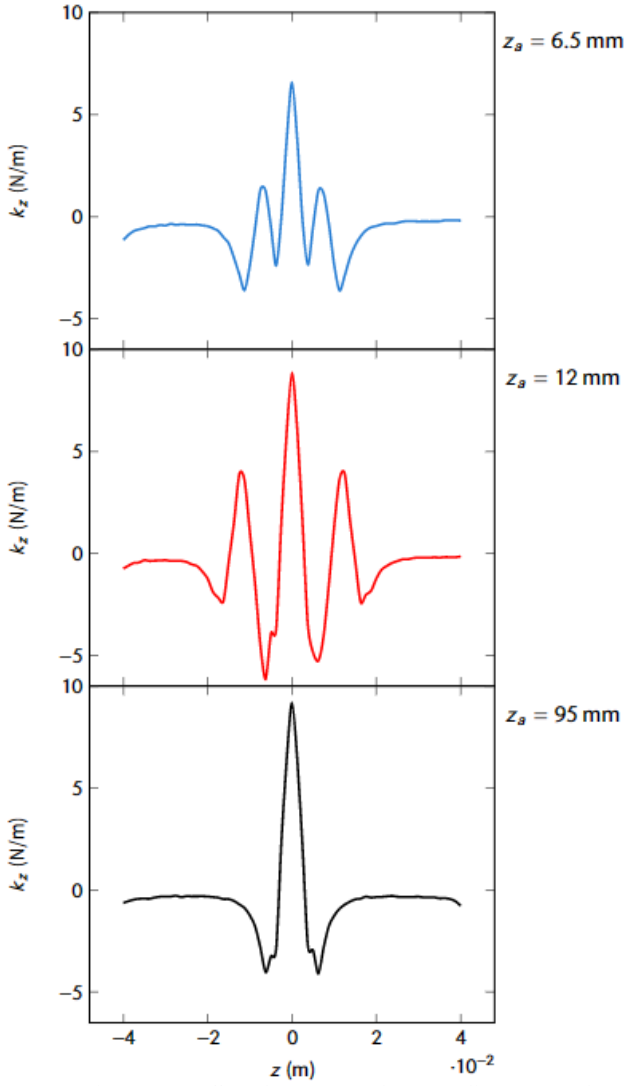

Fig. 12: Axial magnetic stiffness between two diametrically magnetized PMBs as a function of the axial displacement of the inner permanent ring magnets for various z_a *values. It is taken into account for magnets:* $r_a = 26.6$ mm, $r_b = 34.8$ mm, $r_c = 13$ mm, $r_d = 26$ mm, $h = 5$ mm, *and* $M = 10$ kA/m

would be stable there. Instead, the configuration with the maximum value of k_z is $z\_a = 95$ mm, while the configuration with the lowest value is $z_a = 6.5$ mm, showing once again that the proximity of bearings with the same magnetization direction has an effect on stability.

V. Comparison of Two PMB Configurations with Different Magnetization Directions

In this section, the behavior of F_z and k_z of three systems of two PMBs used in ventricular assist devices is compared. These configurations contain two bearings: the first one with axial magnetization (Fig. 13), the second one with radial magnetization (Fig. 14), and the third one with diametrical magnetization (Fig. 7). Remember that in [11] and [12], PMBs with axial and radial magnetization were studied.

In this instance, the FEM was used as a tool to investigate the magnetic force as well as the magnetic stiffness. For the numerical simulations, the magnetic bearings had the following dimensions: $r_a = 26.6$ mm, $r_b = 34.8$ mm, $r_c = 13$ mm, $r_d = 26$ mm, $h = 5$ mm; all magnets have the same magnitude of magnetization, $M = 10$ kA/m; and $z_a = 95$ mm. The configurations differed solely in magnetization direction. Fig. 15 shows the axial component F_z of the magnetic force on the internal magnets of the bearings as a function of axial displacement z for each arrangement. In it, it is observed that F_z has a similar behavior regardless of the magnetization of the

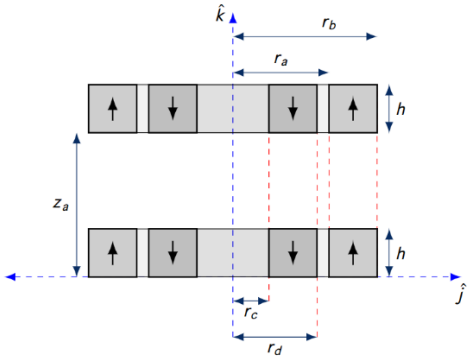

Fig. 13: Configuration of two PMBs with axial magnetization.

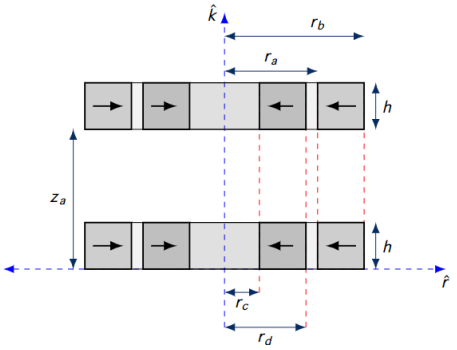

Fig. 14: Configuration of two PMBs with radial magnetization.

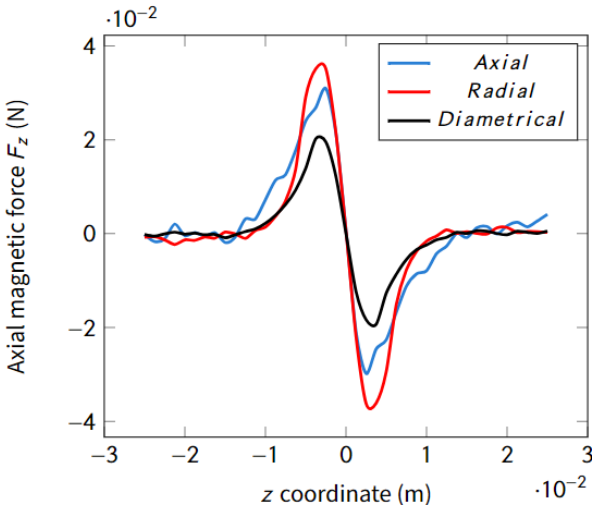

Fig. 15: Axial magnetic force F_z as a function of axial shift z for different PMBs configurations (axial, radial, and diametrical). It is taken into account for magnets: r_a = 26.6 mm, r_b = 34.8 mm, r_c = 13 mm, r_d = 26 mm, h = 5 mm, and M = 10 kA/m.

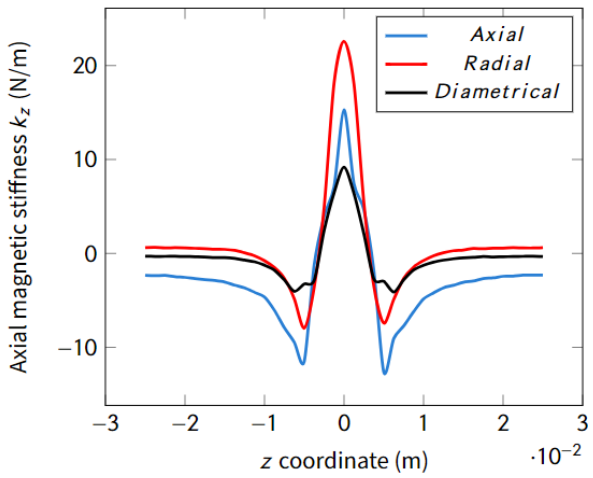

Fig. 16: Axial magnetic stiffness k_z as a function of axial shift z for different PMBs configurations (axial, radial, and diametrical). It is considered for magnets: r_a = 26.6 mm, r_b = 34.8 mm, r_c = 13 mm, r_d = 26 mm, h = 5 mm, and M = 10 kA/m.

bearings, but the significant difference is presented in terms of the maximum (or minimum) values, where it can be seen that the configuration with the highest value was the one with radial magnetization ($F_z = 35.1$ mN), followed by the one with axial magnetization ($F_z = 30.9$ mN) and the configuration with the lowest value was the diametrical ($F_z = 20.2$ mN). The picture also shows that F_z is null for $z < -10$ mm and $z > 10$ mm regardless of magnetization.

Fig. 16 shows how the axial magnetic stiffness k_z changes as a function of the axial displacement z for the different types of PMBs. It can be seen that the k_z curve behaves the same way no matter how the magnets are magnetized, with the difference being in the maximum and minimum values. Radial magnetization ($k_z = 22.6$ N/m) had the greatest value, followed by axial (15.3 N/m) and diametrical (9.18 N/m). According to the results presented in Fig. 15 and Fig. 16, systems made up of radial and axial PMBs are more stable than systems formed by diametric PMBs under the same conditions (size and magnetization).

VI. Conclusions

From this study, the behavior of the axial magnetic stiffness k_z and the axial components of the magnetic force F_z between the internal and external magnets of different configurations of diametrically magnetized PMBs was analyzed.

First, a mathematical model of the magnetic field of a diametrically magnetized annular permanent magnet was found. From this model, the main parameters that define the field were found, as well as the components of the field at a point on the magnet's line of symmetry, which was used as the starting point for the FEM model.

After that, the behavior of k_z and F_z was studied as a function of the axial displacement z for one or two diametrical PMBs, for both configurations, it was found that as r_d increased (making the space between the magnets smaller), so did the values of F_z and k_z. Regarding k_z, it was discovered that regardless of the value of r_d, the maximum stability occurs at $z = 0$ mm, as expected given that F_z is zero at this point. On the other hand, it was found that the range of action of F_z for a PMB was between -10 mm and 10 mm, no matter what r_d was. For two PMBs, this range depends on how far apart the bearings are.

Lastly, it was found that under the same conditions (size and magnetization), diametrical PMBs are less stable and have less axial magnetic force than those of axial or radial PMBs.

Acknowledgments

We are grateful for the assistance of the SIBILA laboratory and the Academic Doctorate Program in Engineering at the Costa Rica Institute of Technology during the project's implementation. We also thank Professor Juan Luis Crespo Mariño for his excellent advice.

References

[1] G. Ortiz-Leon, «Modelo de un nuevo concepto de impulsor para la aplicación en bombas para sangre,» Cartago, 2017.

[2] Z. Weiyu y Z. Huangqiu, «Radial magnetic bearings: An overview,» *Results in physics, Elsevier,* vol. 7, pp. 303--312, 2017.

[3] P. Samanta y H. Hirani, , «On the Evolution of Passive Magnetic Bearings,» *Journal of Tribology,* vol. 144, pp. 2038--2042, 2021.

[4] H. S. Zad , T. I. Khan y I. Lazoglu, «Design and analysis of a novel bearingless motor for a miniature axial flow blood pump,» *{IEEE Transactions on Industrial Electronics,* vol. 65, pp. 4006-4016, 2017.

[5] A. Fenercioglu, «Design and analysis of a magnetically levitated axial flux BLDC motor for a ventricular assist device (VAD),» *Turkish Journal of Electrical Engineering and Computer Sciences,* vol. 24, pp. 2881-2892, 2016.

[6] L. Tompkins, B. Gellman, S. Prina y G. Morello, «Development of inspired therapeutics pediatric vad: computational analysis and characterization of vad v3,» *Cardiovascular Engineering and Technology,* vol. 13, pp. 624--637, 2022.

[7] S. Earnshaw, «On the nature of the molecular forces which regulate the constitution of the luminiferous ether,» *Transactions of the Cambridge Philosophical Society,* vol. 7, p. 97, 1848.

[8] F. Betschon, «Design principles of integrated magnetic bearings,» 2000.

[9] J. P. Yonnet, «Permanent magnet bearings and couplings,» *IEEE Transactions on magnetics,* vol. 17, pp. 1169--1173, 1981.

[10] G. Jungmayr, E. Marth, W. Amrhein, H. J. Berroth y F. Jeske, «Analytical stiffness calculation for permanent magnetic bearings with soft magnetic materials,» *IEEE Transactions on magnetics},* vol. 50, pp. 1-8, 2014.

[11] R. Ravaud, G. Lemarquand y V. Lemarquand, «Force and stiffness of passive magnetic bearings using permanent magnets. Part 1: Axial magnetization,» *{IEEE Transactions on magnetics,* vol. 45, pp. 2996--3002, 2009.

[12] R. Ravaud, G. Lemarquand y V. Lemarquand, «Force and stiffness of passive magnetic bearings using permanent magnets. Part 2: Radial magnetization,» *IEEE Transactions on magnetics,* vol. 45, pp. 3333-3342, 2009.

[13] A. Bolotov, O. Novikova y V. Novikov, «Force interaction of permanent magnets in passive magnetic bearings,» *{AIP Conference Proceedings,* vol. 2526, pp. 2038--2042, 2023.

[14] J. R. Reitz, F. J. Milford y R. W. Christy,, Fundamentos de la teoría electromagnética, 4th ed., Wilmington, Delaware: Addison-Wesley Iberoamericana, S.A., 1996.

[15] V. T. Nguyen y T. F. Lu, «Analytical Expression of the Magnetic Field Created by a Permanent Magnet with Diametrical Magnetization,» *Progress In Electromagnetics Research C,* vol. 87, 2018.

[16] M. Fontana, M. AlizadehTir y M. Bergamasco, «Novel magnetic sensing approach with improved linearity,» *Sensors,* vol. 13, pp. 7618--7632, 2013.

[17] F. Marignetti, F. Salsedo y S. M. Mirimani, «An axial passive magnetic bearing using three PM rings,» *IET Electric Power Applications,* vol. 15, pp. 415--428, 2021.

[18] J. M. Camacho y V. Sosa, «Alternative method to calculate the magnetic field of permanent magnets with azimuthal symmetry,» *Revista mexicana de fisica E,* vol. 59, pp. 8-17, 2013.